


In Vivo Longitudinal ^1H MRS Study of Transgenic Mouse Models of Prion Disease in the Hippocampus and Cerebellum at 14.1 T

Cristina Cudalbu¹  · Melanie Craveiro² · Vladimír Mlynárik¹ · Juliane Bremer³ · Adriano Aguzzi³ · Rolf Gruetter^{1,2,4}

Received: 9 December 2014 / Revised: 5 June 2015 / Accepted: 16 June 2015 / Published online: 23 July 2015
© Springer Science+Business Media New York 2015

Abstract In vivo ^1H MR spectroscopy allows the non-invasive characterization of brain metabolites and it has been used for studying brain metabolic changes in a wide range of neurodegenerative diseases. The prion diseases form a group of fatal neurodegenerative diseases, also described as transmissible spongiform encephalopathies. The mechanism by which prions elicit brain damage remains unclear and therefore different transgenic mouse models of prion disease were created. We performed an in vivo longitudinal ^1H MR spectroscopy study at 14.1 T with the aim to measure the neurochemical profile of Prnp^{-/-} and PrP $_{\Delta 32-121}$ mice in the hippocampus and cerebellum. Using high-field MR spectroscopy we were able to analyze in details the in vivo brain metabolites in Prnp^{-/-} and PrP $_{\Delta 32-121}$ mice. An increase of myo-inositol, glutamate and lactate concentrations with a decrease of N-acetylaspartate concentrations were observed providing additional information to the previous measurements.

Keywords In vivo proton magnetic resonance spectroscopy · Brain metabolites · Mouse brain · Prion disease

Introduction

Prion diseases form a group of fatal neurodegenerative diseases, also described as transmissible spongiform encephalopathies (TSEs), which are caused by abnormal conformational isomers (PrP^{Sc}) of the host-encoded prion proteins (PrP^C) [1]. PrP^C is expressed in all vertebrate species examined to date, mainly in the brain but also in many other tissues at lower levels [2]. The nature of the prion has been a longstanding enigma. Both, the physiological function of PrP^C and the molecular pathways leading to neurodegeneration in prion disease remain unknown. In addition, the mechanism by which prions elicit brain damage and the relative contributions of PrP^{Sc} accumulation and PrP^C depletion to the prion replication remains unclear [3].

Consequently, different animal models were created to study the role of the PrP^C. Among these models, knockout mouse models were crucial in elucidating the precursor-product relationship between PrP^C and PrP^{Sc}. Among these models, the mice lacking prion protein (Prnp^{-/-}) developed normally and no severe pathologies were observed [4]. In contrast, mice expressing PrP which lacks defined domains (PrP $_{\Delta 32-121}$) suffer from ataxia, astrogliosis and cerebellar granule cell loss [5]. Since the lack of PrP^C itself did not induce an obvious phenotype, mice expressing PrP, which lacks defined domains, may allow the identification of functionally relevant domains within PrP^C. Generally, prion diseases in humans (also called Creutzfeldt–Jakob disease) are characterized by neurodegeneration with primary signs

Special Issue: In Honor of Dr. Gerald Dienel.

✉ Cristina Cudalbu
cristina.cudalbu@epfl.ch

- ¹ Centre d’Imagerie Biomedicale, Ecole Polytechnique Fédérale de Lausanne (EPFL), Lausanne, Switzerland
- ² Laboratory for Functional and Metabolic Imaging (LIFMET), Ecole Polytechnique Fédérale de Lausanne (EPFL), Lausanne, Switzerland
- ³ Institute of Neuropathology, University Hospital of Zurich, Zurich, Switzerland
- ⁴ Departments of Radiology, Universities of Lausanne and Geneva, Lausanne, Switzerland

of impaired cognitive functions and ataxia [6]. Moreover, the neuropathological features are spongiform degeneration of the brain accompanied by neuronal loss and astrocytic activation (gliosis) [6]. These findings accentuate the need for a non-invasive and longitudinal investigation technique which could bring additional information.

Magnetic resonance imaging (MRI) and magnetic resonance spectroscopy (MRS) became in the last decades powerful and reliable diagnostic tools allowing the non-invasive characterization of brain metabolites together with the study of brain metabolites changes in a wide range of neurodegenerative diseases. In addition, the availability of high magnetic field strengths (≥ 7 T) combined with the possibility of acquiring spectra at very short echo time (< 10 ms) have increased the number of in vivo detectable brain metabolites to about 20 metabolites in animal models and humans: glucose (Glc), lactate (Lac), creatine (Cr), phosphocreatine (PCr), alanine (Ala) (markers of energy metabolism); phosphocholine (PCho), glycerophosphocholine (GPC), phosphoethanolamine (PE), N-acetylaspartate (NAA), N-acetylaspartylglutamate (NAAG) (markers of myelination/cell proliferation); glutamate (Glu), glutamine (Gln), aspartate (Asp), γ -aminobutyrate (GABA), glycine (Gly) (neurotransmitters and associated metabolites); taurine (Tau), myo-inositol (Ins) (markers of osmoregulation) and ascorbate (Asc), glutathione (GSH) (antioxidants). Consequently, the use of in vivo, non-invasive and longitudinal MR measurements is a promising tool to assess pathogenic mechanisms, to diagnose and monitor disease progression and/or effect of treatment, and made a bridge between the clinical diagnostics and basic research.

Only few reports describe the use of in vivo ^1H MRS in patients with prion disease so far [7–11]. This number is even smaller for animal models [12–14]. In addition, only a few metabolites were reported in these studies (mainly NAA).

To our knowledge, no in vivo MRS study was performed in transgenic mouse models of prion disease. Therefore, the aim of the present study was to measure the neurochemical profile of Prnp $-/-$ and PrP $_{\Delta 32-121}$ mice in the hippocampus and cerebellum at 6 and 12 months of age using in vivo longitudinal ^1H MRS at 14.1 T.

Methods

Animals

Mice lacking prion protein (Prnp $-/-$ mice, $n = 6$) and mice expressing PrP which lacks defined domains (PrP $_{\Delta 32-121}$, $n = 6$) were created in the laboratory of Prof A. Aguzzi in Zurich as described in ref [4] and [5], respectively. Six wild type mice (WT) were used as controls. All the mice used in

this study were of BALB/c strain. In vivo MRI and MRS experiments were performed longitudinally at 6 and 12 months of age on all the animals (total of 18 mice). Spontaneously breathing mice were anesthetized during experiments with 1.3–1.5 % isoflurane in oxygen (Attane, Minrad, NY, USA) using a nose mask. A stereotaxic system (bite bar and a pair of ear bars) (Rapid Biomedical, Germany) was used to fix the head. Then the animal was placed in an in-house-built holder and afterwards placed in the magnet. The vital signs of the animals were carefully monitored during in vivo measurements to provide a stable physiological condition. Body temperature was measured using a rectal thermosensor and maintained at 36.5 ± 0.2 °C by circulating warm water around the animals. Respiration rate was monitored by a small-animal monitor system (SA Instruments Inc., New York, NY, USA).

All MRI and MRS experiments were conducted according to federal and local ethical guidelines and the protocols were approved by the local regulatory body of the Canton Vaud, Switzerland.

MRI and MRS Measurements

All data were acquired on a 14.1 T/26 cm system (Magnex Scientific, Oxford, UK) interfaced to a Varian Direct Drive console (Palo Alto, CA, USA) and equipped with 12-cm inner-diameter actively-shielded gradient set with a maximum gradient of 400 mT/m in 120 μs . A home-built quadrature coil consisting of two geometrically decoupled 14-mm-diameter single loops was used as radio frequency (RF) transceiver. Eddy currents were minimized using time-dependent quantitative eddy-current field mapping [15]. The static field was shimmed using first- and second order shims obtained by the echo planar imaging (EPI) version of FASTMAP [16]. First, T_2 weighted images were obtained in the axial plane using a multislice fast spin echo protocol with $\text{TR}/\text{TE}_{\text{eff}} = 5000/52$ ms; echo train length = 8; field-of-view = 24 mm \times 24 mm; slice thickness = 0.6 mm; 6 averages; 128 \times 128 image matrix. Afterwards, ^1H MRS spectra were acquired using the ultra-short-echo time SPECIAL spectroscopy sequence ($\text{TE} = 2.8$ ms, $\text{TR} = 4$ s, 400 scans) [17]. A VOI of $1.3 \times 2 \times 2.2$ mm 3 was selected in the hippocampus and a second VOI of $2 \times 2.5 \times 2$ mm 3 was selected in the cerebellum. After first and second order shimming, the typical linewidth of water resonance at $\text{TE} = 2.8$ ms was 18–23 Hz. The water signal was suppressed using the VAPOR module containing a series of seven 25 ms asymmetric variable power RF pulses with optimized relaxation delays [18]. To improve the signal localization, three modules of outer volume saturation (OVS) were interleaved with the water suppression pulses as described previously [18]. Spectra were collected in blocks of 16 averages to compensate for the magnetic field drift.

The blocks were stored separately in the memory and corrected for the relative shift in frequency and potential variations in phase before summation using an in house matlab routine.

Metabolite concentrations were estimated using LCModel (<http://s-provencher.com/pages/lcmodel.shtml>) [19], combined with a quantum mechanics simulated basis-set of metabolites based on the density-matrix formalism, and using published values of J-coupling constants and chemical shifts [20]. The following 20 metabolites were included in the basis-set: Ala, Asp, PCho, Cr, PCr, GABA, Gln, Glu, GSH, Gly, Ins, Lac, NAA, Tau, Asc, Glc, NAAG, GPC, Scyllo (scyllo-inositol) and PE. LCModel is also reporting the sum of selected metabolites like tNAA (NAA + NAAG), tCho (PCho + GPC) and tCr (Cr + PCr) but these are not considered as being additional estimated metabolites. In addition, the spectrum of macromolecules measured in vivo as described previously [17, 21–23] was included in the basis-set. Absolute metabolite concentrations were obtained using unsuppressed water signal as an internal reference. The Cramer–Rao lower bounds were used as a reliability measure of the metabolite concentration estimates.

All metabolite concentrations are presented as mean \pm SD. Significance for difference was tested using a

two-way repeated measures ANOVA followed by Bonferroni post-test (Prism 5, GraphPad, La Jolla, CA, USA). Probability values of $p < 0.05$ were considered statistically and biologically significant. ANOVA between prion and WT mice was performed with respect to metabolite in the neurochemical profile in each brain region with age as repeated factor.

Results

To evaluate the consistency of our data on WT mice with prior literature we analyzed the brain regional differences between hippocampus and cerebellum together with the age dependency (6 vs 12 months of age). Substantial regional variations (hippocampus vs cerebellum) were obtained and were also visually discernible after a careful inspection of the spectra (Fig. 1): an increase in Tau ($p < 0.001$) peak and lower Ins ($p < 0.05$), tCr ($p < 0.05$) signal intensities. These regional differences are similar with previously published data in another mouse strain, the C57BL/6 mice [24]. For both brain regions the metabolite concentrations are very similar at both ages. The only change with age was found in hippocampus: a decrease in Ins ($p < 0.05$) and tCho ($p < 0.05$) concentrations.

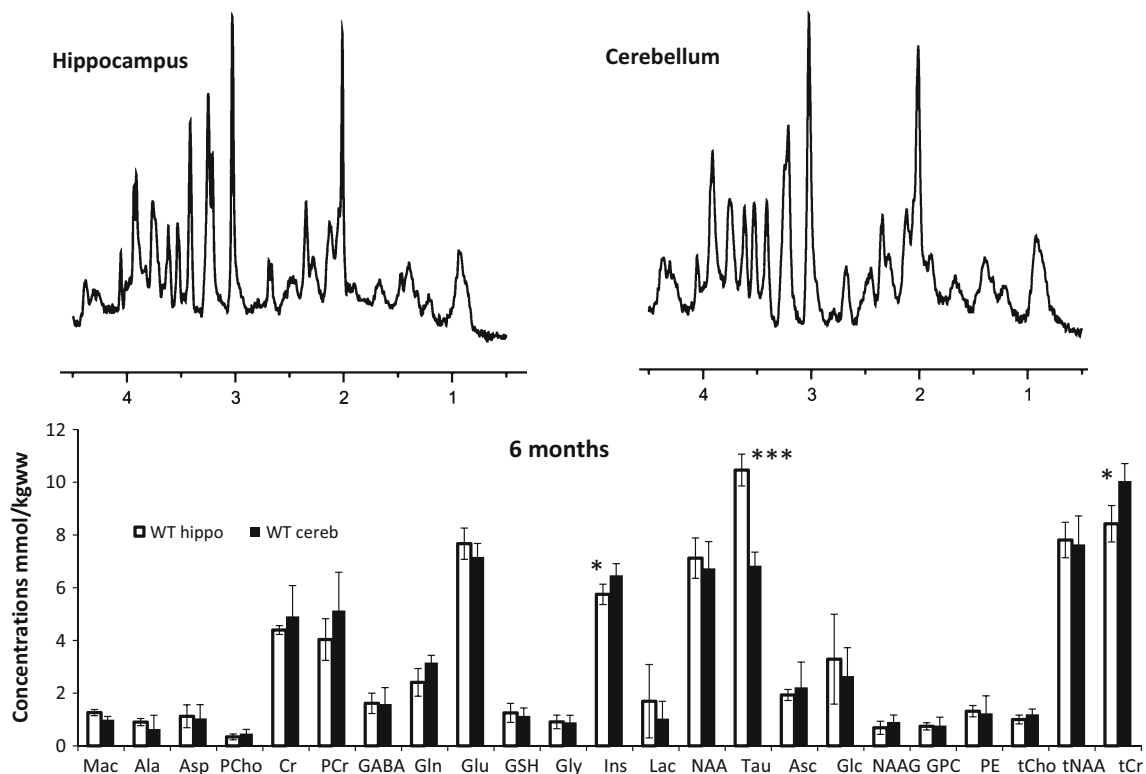


Fig. 1 Up in vivo ^1H MRS spectra acquired in the hippocampus and cerebellum of a WT mouse using the SPECIAL sequence, down the neurochemical profile (mean \pm SD) in the hippocampus and cerebellum of 6-month old WT mice

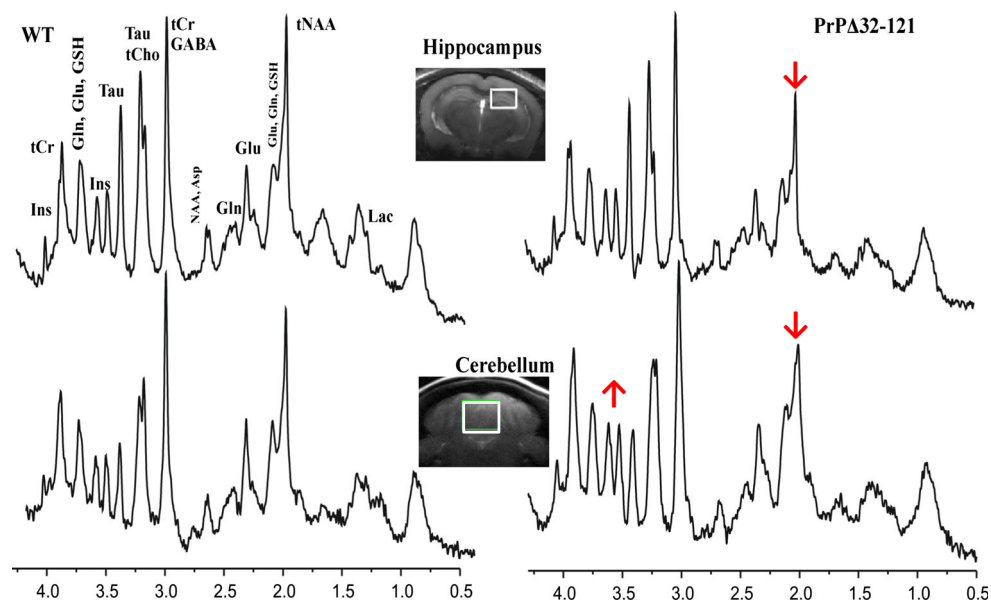


Fig. 2 SPECIAL ^1H spectra (TE = 2.8 ms, TR = 4000 ms) and voxel localization acquired at the age of 12 months in the hippocampus and cerebellum of a WT and PrP $_{\Delta 32-121}$ mouse. Differences in

relative intensities are visible in the spectra and marked with arrows (i.e. decreased NAA and increased Ins peaks)

No visible difference in the T_2 weighted images was observed between the WT and Prnp $-/-$ or PrP $_{\Delta 32-121}$ animals. The T_2 weighted images showed adequate anatomical contrast and spatial resolution for accurate positioning of the voxel in hippocampus and cerebellum based on anatomical landmarks (Fig. 2).

To assess the quality of in vivo ^1H MRS data Figs. 1, 2 and 4 show the high quality spectra obtained routinely in our study. In general, spectra exhibited excellent signal-to-noise ratio estimated by LCModel as the ratio of the maximum in the spectrum minus baseline over the analysis window to twice the root-mean-square residuals (i.e. 19 ± 3 for hippocampus and 26 ± 4 for cerebellum, Figs. 1 and 2). The VAPOR water suppression provided a residual water signal intensity below that of NAA and the quality of signal localization was confirmed by the absence of contamination with extracerebral lipid peaks at 1.3–1.7 ppm. In our study, FASTMAP shimming resulted in unsuppressed water signal linewidths of 18–20 Hz for hippocampus and 20–23 Hz for cerebellum, which leads to highly resolved spectra. Moreover, notable differences in metabolite signals were discernible directly from the spectra (a decrease of NAA and an increase of Ins peaks) as shown in Figs. 1, 2 and 4.

To determine potential differences between Prnp $-/-$, WT and PrP $_{\Delta 32-121}$ mice, the neurochemical profile (mean \pm SD) measured at 12 months in the hippocampus and cerebellum is shown in Fig. 3. We were able to reliably estimate the concentration of 19 brain metabolite with CRLBs between 1 and 20 %. The signal of scyllo-inositol

was included in the basis-set but its concentration was not reliably estimated in the majority of the spectra (CRLBs > 55 %).

The PrP $_{\Delta 32-121}$ mice showed no significant changes in the hippocampus at 6 months; however an increase of Ins (15 %, $p < 0.05$) and Glu (20 %, $p < 0.05$) was found in the cerebellum (data not shown). At 12 months we observed decrease of NAA (20 %, $p < 0.05$) in both hippocampus and cerebellum, which was clearly visible in the spectra (Fig. 2). The increase in Ins noticed in the cerebellum at 6 months was also observed at 12 months (17 %, $p < 0.05$). This increase is also discernible in the spectra presented in Fig. 2.

In the Prnp $-/-$ mice at 6 months of age, the overall neurochemical profile was similar to the WT in the hippocampus and cerebellum (data not shown). However, at 12 months of age an increase of Glu (30 %, $p < 0.001$), Ins (20 %, $p < 0.01$), and Lac (100 %, without reaching statistically significance) was found in the hippocampus (Fig. 4). An increase of Lac (100 %, $p < 0.05$) was also observed in the cerebellum.

Discussion

To the best of our knowledge, this is the first study evaluating the neurochemical profile of transgenic mouse models of prion disease. In the present study, the high quality data obtained in vivo at 14.1 T was evident from the high signal to noise ratio signal-to-noise ratio, excellent

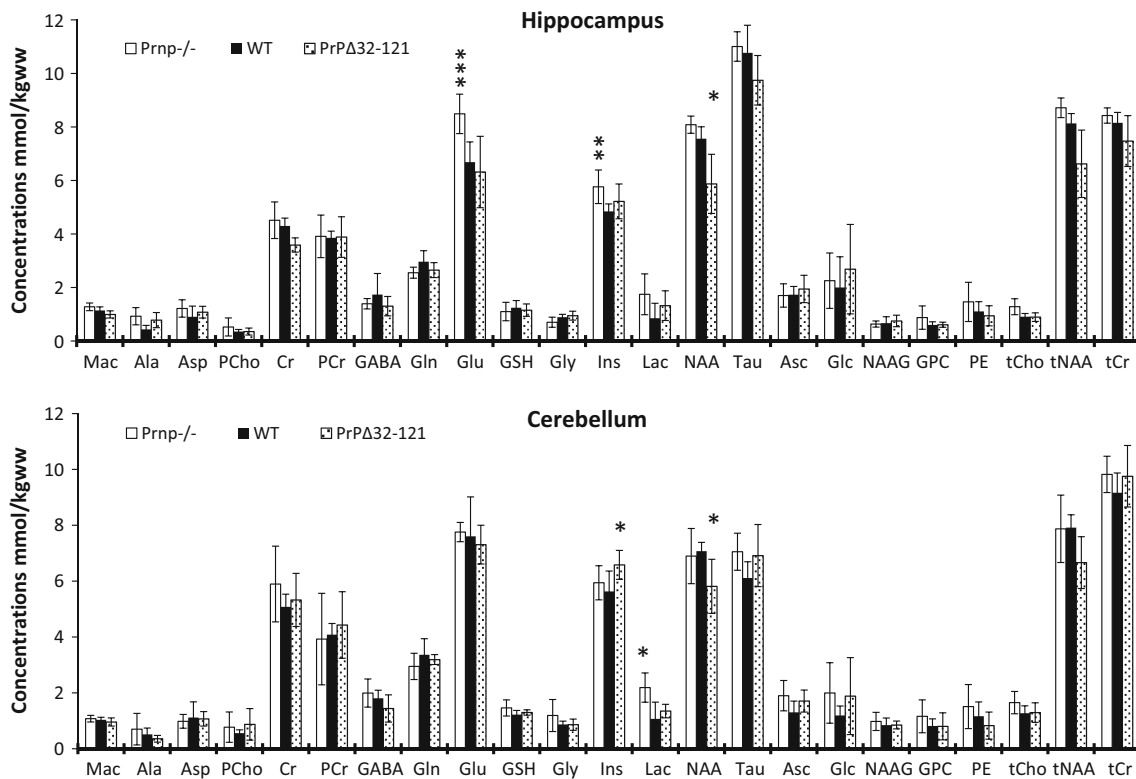


Fig. 3 Neurochemical profile (mean ± SD) in the hippocampus (H) and cerebellum (C) of Prnp *-/-*, WT and PrP Δ_{32-121} mice at 12 months of age

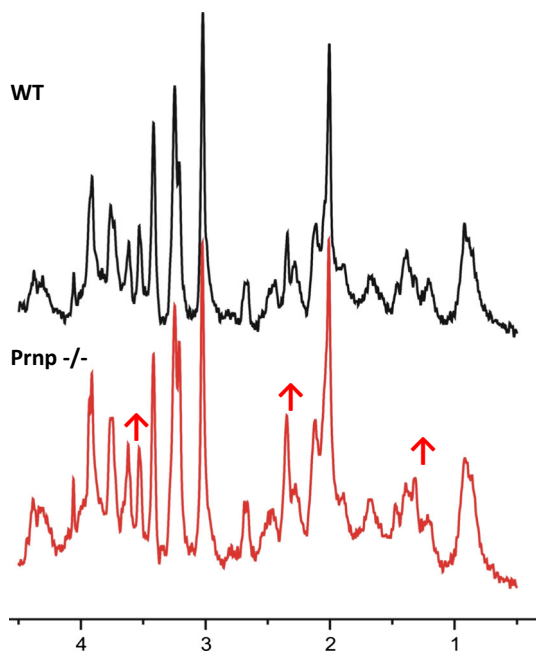


Fig. 4 Representative ^1H MRS spectra acquired in the hippocampus of a WT and Prnp *-/-* mouse at 12 months of age using the SPECIAL sequence (TE = 2.8 ms, TR = 4000 ms)

water suppression, localization performance and spectral resolution. In addition, the ultra-short echo time used during our acquisitions (TE = 2.8 ms) combined with a reliable quantification algorithm allowed the quantification of 19 metabolites in the hippocampus and cerebellum of 6 and 12 months old Prnp *-/-* and PrP Δ_{32-121} mice and thus substantial metabolic information was obtained in prion disease.

In the mouse brain, ^1H MRS can be technically rather challenging due to its small size, especially if spectra are acquired in a small brain region, which is, in addition, located close to the interface between the diamagnetic tissue and air containing paramagnetic oxygen. Moreover, magnetic field inhomogeneities induced in the brain by the difference in susceptibility on air/tissue interface are scaled linearly with B $_0$, thus leading to increased peak linewidths (in Hz). In our study, the high quality of mouse brain spectra was achieved due to shimming with FASTMAP and also due to high signal intensity provided by the spin-echo full intensity localization technique (SPECIAL) in a scan time of 25 min. The water linewidths were comparable with previously published mouse data [24, 25], with slightly larger water linewidths in the cerebellum compared to hippocampus. This is mainly due to the fact that the

cerebellum has higher microscopic heterogeneity but also due to its location (closer to the neck with a potentially higher risk of movement).

To the best of our knowledge, very few ^1H MRS studies were performed *in vivo* on humans or mice models injected with CJD (Creutzfeldt–Jakob) or scrapie agent (ME7 strain). All these previous studies were done at low magnetic field and only a few metabolites were measured (i.e. NAA, tCr, tCho, and sometimes Ins) and mainly metabolite ratios were reported and not absolute concentrations [7–14]. These studies reported changes in Ins and NAA concentrations. The decrease of NAA was reported to reflect neuronal stress and death whereas the increase of Ins an indicator of astrogliosis.

Previously published studies on the Prnp $-/-$ mice showed that these mice develop and reproduce normally and show no detectable physical or behavioral defect together with no apparent immunological changes for at least 7 months [4]. Moreover, when inoculated with mouse scrapie prions they remain free of scrapie symptoms for 13 months in contrast to wild-type controls which died after at 6 months of age [26], suggesting that PrP^c is required for the usual susceptibility to scrapie and that the lack of homology between incoming prions and the host's PrP genes inhibits the disease. Phenotypic defects in these knockout mice suggested a role of PrP^c in maintaining normal circadian rhythms, superoxide dismutase activity and protection from oxidative stress and copper metabolism [27–29]. More recent studies on mice lacking prion protein prepared in another laboratory showed significant age-related defects in motor coordination and balance together with spongiform pathology and reactive astrocytic gliosis on brain analysis which normally characterize prion disease [3].

In addition to the previously mentioned studies, our study characterized the brain metabolites *in vivo* and longitudinally in Prnp $-/-$ mice using ^1H MRS and reported the concentration of 19 brain metabolites providing substantial metabolic information. Among these metabolites only Glu, and Ins showed significant changes in hippocampus at 12 months of age, whereas no changes being measured at 6 months of age.

Glutamate is an important amino acid present in the brain at high concentrations (see Fig. 3) and a major excitatory neurotransmitter [30]. Changes in glutamate levels were linked to a dysfunction in the neurotransmission or to metabolic activity (Krebs cycle) with increases of glutamate concentration being related to increased metabolic activity [30]. In addition, we have computed the Gln/Glu ratios and found a 30 % decrease compared with the WT animals at 12 months of age. Brain glutamine is exclusively synthesized in glial cells, through the glutamine synthetase enzyme [31], from glutamate cleared

from the synaptic cleft, thus having a major role in neurotransmission. Then this glutamine is shuttled to neurons where it can be deaminated, completing the so-called glutamate–glutamine cycle [32, 33]. Therefore, Gln/Glu ratios may reflect glutamate–glutamine cycle activity between neurons and glial cells.

The roles of Ins in the brain are not fully understood, however, it is accepted to be a major osmolyte involved in the maintenance of cell volume. It is also a constituent of phosphoglycerides and consequently lipid component of biomembranes and a major component of intracellular second messenger system [30]. Reduced concentrations of Ins have been linked to a response to an osmotic stress [34, 37] while increased concentrations, which appear to be more specific for neurodegenerative diseases, were believed to reflect increased population of glial cells based on the hypothesis that Ins is expressed in high amounts in glial cells [35]. Our findings of increased Ins in the hippocampus at 12 months seems to be potentially linked to astrogliosis, in agreement with the histological results obtained previously on Prnp $-/-$ mice [3] and on humans or mice models injected with scrapie agent [7, 14]. To date, the *in vivo* modifications in Glu and Lac concentrations have never been reported in Prnp $-/-$ mice.

On the other hand, PrP _{Δ 32–121} mice were shown to develop ataxia and neuronal death, which were limited to the granular layer of the cerebellum, as early as in 1–3 months old animals [5]. Our measurements showed that the most important modifications in the brain metabolites appeared mainly at 12 months of age in both hippocampus and cerebellum (decreased NAA and increased Ins), even though we also detected significant changes at 6 months of age in these mice (increased Ins and Glu). The increase of Ins in the cerebellum at 6 and 12 months may reflect astrogliosis related to an inflammatory process, consistent with the histological features [5]. Since the role of Ins as a glial marker is sometimes disputed, we analyzed the linear correlation with glutamine only at 12 months of age and detected a linear relation with $R^2 = 0.6$. Glutamine synthetase enzyme, predominately located in astrocytes [31] although it may also be expressed in neurons under certain pathological conditions [30], is responsible for the synthesis of glutamine from glutamate cleared from the synaptic cleft. Glutamine synthetase is also the major pathway for ammonia detoxification [34, 36, 37].

NAA is found in high concentrations in the brain and is generally considered as a neuronal marker based on previous studies showing that brain tumors of glial origin did not contain NAA [30, 38]. Later on, NAA was also localized in immature oligodendrocytes using cultured cells [39]. From studies of neurodegenerative conditions, NAA was suggested to be a marker of neuronal density while others consider NAA more as a marker of neuronal

function since NAA was shown to recover following stroke, mitochondrial disorders and multiple sclerosis [30, 40–42]. In our study, the decrease in NAA was shown to appear at the end stage of the disease (i.e. in 12 months old mice) and it seems to reflect neuronal loss in agreement with the histological findings [5] and with the studies performed post-mortem in humans. Since glutamate is considered to be mainly located in neurons [32, 33] (even though sometimes this assumption needs to be taken with care [30]), we have plotted the linear correlation between NAA and Glu at 12 months of age and found a good correlation with $R^2 = 0.57$.

Finally, when comparing the brain metabolites changes measured in Prnp *-/-* mice to those in PrP_{Δ32-121} mice we can notice that modifications were obtained mainly at 12 months of age in both models with some modifications already noticeable at 6 months of age only in the cerebellum of PrP_{Δ32-121} mice (increase of Ins and Glu). Moreover, Prnp *-/-* mice showed stronger modifications in the hippocampus (increase of Ins and Glu) than in the cerebellum (increase of Lac), while PrP_{Δ32-121} mice showed a decrease of NAA in both brain regions and an increase of Ins only in the cerebellum. The increase in Ins observed in both mouse models is consistent with the observations made in human prion disease reflecting astrogliosis. From histological point of view, while the Prnp *-/-* mice used in our study developed normally with no severe pathology [4], the Prnp *-/-* mice prepared in another laboratory showed very similar characteristics to the human disease (i.e. age-related defects in motor coordination and balance together with spongiform pathology and reactive astrocytic gliosis in globus pallidus and cerebellum [3]). The PrP_{Δ32-121} mice suffer from ataxia and seem to have different pathology from prion infections characterized by astrogliosis and cerebellar granule cell loss mainly in the cerebellum [5], even though our measurements showed modifications which are very similar to the human prion disease (decrease NAA in both hippocampus and cerebellum and increased Ins in cerebellum). In addition, some recent transcriptomic analyses showed that there is considerable overlap between the mice used in our study, the exposure to antibodies targeting the cellular prion protein and the pathologies related to prions, namely prion infections [43, 44].

We conclude that high-field MR spectroscopy allows to analyze in detail the concentrations of 19 brain metabolites in Prnp *-/-* and PrP_{Δ32-121} mice and consequently provides additional information to the previous behavioral and histological measurements.

Acknowledgments Supported by Centre d’Imagerie BioMédicale (CIBM) of the UNIL, UNIGE, HUG, CHUV, EPFL, the Leenaards and Jeantet Foundations. The authors thank Dr Frédéric Schütz (Biostatistics Service, Bioinformatics Core Facility, SIB Swiss Institute of Bioinformatics) for the discussions regarding the statistics.

References

- Prusiner SB (1991) Molecular biology of prion diseases. *Science* 252(5012):1515–1522
- Bendheim PE, Brown HR, Rudelli RD, Scala LJ, Goller NL, Wen GY, Kascak RJ, Cashman NR, Bolton DC (1992) Nearly ubiquitous tissue distribution of the scrapie agent precursor protein. *Neurology* 42(1):149–156
- Nazor KE, Seward T, Telling GC (2007) Motor behavioral and neuropathological deficits in mice deficient for normal prion protein expression. *Biochim Biophys Acta* 1772(6):645–653. doi:10.1016/j.bbadis.2007.04.004
- Bueler H, Fischer M, Lang Y, Bluethmann H, Lipp HP, DeArmond SJ, Prusiner SB, Aguet M, Weissmann C (1992) Normal development and behaviour of mice lacking the neuronal cell-surface PrP protein. *Nature* 356(6370):577–582. doi:10.1038/356577a0
- Shmerling D, Hegyi I, Fischer M, Blattler T, Brandner S, Gotz J, Rulicke T, Flechsig E, Cozzio A, von Mering C, Hangartner C, Aguzzi A, Weissmann C (1998) Expression of amino-terminally truncated PrP in the mouse leading to ataxia and specific cerebellar lesions. *Cell* 93(2):203–214. doi:10.1016/S0092-8674(00)81572-X
- Aguzzi A, Baumann F, Bremer J (2008) The prion’s elusive reason for being. *Annu Rev Neurosci* 31:439–477. doi:10.1146/annurev.neuro.31.060407.125620
- Cordery RJ, MacManus D, Godbolt A, Rossor MN, Waldman AD (2006) Short TE quantitative proton magnetic resonance spectroscopy in variant Creutzfeldt–Jakob disease. *Eur Radiol* 16(8):1692–1698. doi:10.1007/s00330-005-0090-4
- Galanaud D, Haik S, Linguraru MG, Ranjeva JP, Faucheux B, Kaphan E, Ayache N, Chiras J, Cozzone P, Dormont D, Brandel JP (2010) Combined diffusion imaging and MR spectroscopy in the diagnosis of human prion diseases. *AJNR Am J Neuroradiol* 31(7):1311–1318. doi:10.3174/ajnr.A2069
- Kim JH, Choi BS, Jung C, Chang Y, Kim S (2011) Diffusion-weighted imaging and magnetic resonance spectroscopy of sporadic Creutzfeldt–Jakob disease: correlation with clinical course. *Neuroradiology* 53(12):939–945. doi:10.1007/s00234-010-0820-4
- Pandya HG, Coley SC, Wilkinson ID, Griffiths PD (2003) Magnetic resonance spectroscopic abnormalities in sporadic and variant Creutzfeldt–Jakob disease. *Clin Radiol* 58(2):148–153. doi:10.1053/crad.2002.1080
- Waldman AD, Cordery RJ, MacManus DG, Godbolt A, Collinge J, Rossor MN (2006) Regional brain metabolite abnormalities in inherited prion disease and asymptomatic gene carriers demonstrated in vivo by quantitative proton magnetic resonance spectroscopy. *Neuroradiology* 48(6):428–433. doi:10.1007/s00234-006-0068-1
- Broom KA, Anthony DC, Lowe JP, Griffin JL, Scott H, Blamire AM, Styles P, Perry VH, Sibson NR (2007) MRI and MRS alterations in the preclinical phase of murine prion disease: association with neuropathological and behavioural changes. *Neurobiol Dis* 26(3):707–717. doi:10.1016/j.nbd.2007.04.001
- Bell JD, Cox IJ, Williams SC, Belton PS, McConnell I, Hope J (1991) In vivo detection of metabolic changes in a mouse model of scrapie using nuclear magnetic resonance spectroscopy. *J Gen Virol* 72(Pt 10):2419–2423
- Behar KL, Boucher R, Fritch W, Manuelidis L (1998) Changes in N-acetylaspartate and myo-inositol detected in the cerebral cortex of hamsters with Creutzfeldt–Jakob disease. *Magn Reson Imaging* 16(8):963–968. doi:10.1016/S0730-725X(98)00109-X
- Terpstra M, Andersen PM, Gruetter R (1998) Localized eddy current compensation using quantitative field mapping. *J Magn Reson* 131(1):139–143. doi:10.1006/jmre.1997.1353

16. Gruetter R, Tkac I (2000) Field mapping without reference scan using asymmetric echo-planar techniques. *Magn Reson Med* 43(2):319–323. doi:10.1002/(SICI)1522-2594(200002)43:2<319:AID-MRM22>3.0.CO;2-1
17. Mlynarik V, Cudalbu C, Xin L, Gruetter R (2008) ¹H NMR spectroscopy of rat brain in vivo at 14.1 Tesla: improvements in quantification of the neurochemical profile. *J Magn Reson*. doi:10.1016/j.jmr.2008.06.019
18. Tkac I, Starcuk Z, Choi IY, Gruetter R (1999) In vivo ¹H NMR spectroscopy of rat brain at 1 ms echo time. *Magn Reson Med* 41(4):649–656. doi:10.1002/(SICI)1522-2594(199904)41:4<649:AID-MRM22>3.0.CO;2-G
19. Provencher SW (2001) Automatic quantitation of localized in vivo ¹H spectra with LCModel. *NMR Biomed* 14(4):260–264. doi:10.1002/nbm.698
20. Govindaraju V, Young K, Maudsley AA (2000) Proton NMR chemical shifts and coupling constants for brain metabolites. *NMR Biomed* 13(3):129–153. doi:10.1002/1099-1492(200005)13:3<129:AID-NBM619>3.0.CO;2-V
21. Cudalbu C, Mlynarik V, Gruetter R (2012) Handling macro-molecule signals in the quantification of the neurochemical profile. *J Alzheimers Dis* 31(Suppl 3):S101–S115. doi:10.3233/JAD-2012-120100
22. Cudalbu C, Mlynarik V, Xin L, Gruetter R (2009) Quantification of in vivo short echo-time proton magnetic resonance spectra at 14.1 T using two different approaches of modelling the macromolecule spectrum. *Meas Sci Technol* 20(10):104034. doi:10.1088/0957-0233/20/10/104034
23. Pfeuffer J, Tkac I, Provencher SW, Gruetter R (1999) Toward an in vivo neurochemical profile: quantification of 18 metabolites in short-echo-time (¹H) NMR spectra of the rat brain. *J Magn Reson* 141(1):104–120. doi:10.1006/jmre.1999.1895
24. Tkac I, Henry PG, Andersen P, Keene CD, Low WC, Gruetter R (2004) Highly resolved in vivo ¹H NMR spectroscopy of the mouse brain at 9.4 T. *Magn Reson Med* 52(3):478–484. doi:10.1002/mrm.20184
25. Lei H, Poitry-Yamate C, Preitner F, Thorens B, Gruetter R (2010) Neurochemical profile of the mouse hypothalamus using in vivo ¹H MRS at 14.1 T. *NMR Biomed* 23(6):578–583. doi:10.1002/nbm.1498
26. Bueler H, Aguzzi A, Sailer A, Greiner RA, Autenriep P, Aguet M, Weissmann C (1993) Mice devoid of PrP are resistant to scrapie. *Cell* 73(7):1339–1347. doi:10.1016/0092-8674(93)90360-3
27. Tobler I, Gaus SE, Deboer T, Achermann P, Fischer M, Rulicke T, Moser M, Oesch B, McBride PA, Manson JC (1996) Altered circadian activity rhythms and sleep in mice devoid of prion protein. *Nature* 380(6575):639–642. doi:10.1038/380639a0
28. Brown DR, Besinger A (1998) Prion protein expression and superoxide dismutase activity. *Biochem J* 334(Pt 2):423–429
29. Brown DR, Qin K, Herms JW, Madlung A, Manson J, Strome R, Fraser PE, Kruck T, von Bohlen A, Schulz-Schaeffer W, Giese A, Westaway D, Kretzschmar H (1997) The cellular prion protein binds copper in vivo. *Nature* 390(6661):684–687. doi:10.1038/37783
30. Rae CD (2014) A guide to the metabolic pathways and function of metabolites observed in human brain H-1 magnetic resonance spectra. *Neurochem Res* 39(1):1–36. doi:10.1007/s11064-013-1199-5
31. Norenberg MD, Martinez-Hernandez A (1979) Fine structural localization of glutamine synthetase in astrocytes of rat brain. *Brain Res* 161(2):303–310. doi:10.1016/0006-8993(79)90071-4
32. McKenna MC (2007) The glutamate–glutamine cycle is not stoichiometric: fates of glutamate in brain. *J Neurosci Res* 85(15):3347–3358. doi:10.1002/Jnr.21444
33. Gruetter R (2004) Principles of the measurement of neuroglial metabolism using in vivo ¹³C NMR spectroscopy. *Adv Mol Cell Biol* 31:409–433
34. Cudalbu C (2013) In vivo studies of brain metabolism in animal models of hepatic encephalopathy using H-1 magnetic resonance spectroscopy. *Metab Brain Dis* 28(2):167–174. doi:10.1007/s11011-012-9368-9
35. Brand A, Richterlandsberg C, Leibfritz D (1993) Multinuclear Nmr-studies on the energy-metabolism of glial and neuronal cells. *Dev Neurosci-Basel* 15(3–5):289–298. doi:10.1159/000111347
36. Braissant O, McLin VA, Cudalbu C (2013) Ammonia toxicity to the brain. *J Inher Metab Dis* 36(4):595–612. doi:10.1007/s10545-012-9546-2
37. Cudalbu C, Lanz B, Duarte JM, Morgenthaler FD, Pilloud Y, Mlynarik V, Gruetter R (2012) Cerebral glutamine metabolism under hyperammonemia determined in vivo by localized (¹H and (¹⁵N) NMR spectroscopy. *J Cereb Blood Flow Metab* 32(4):696–708. doi:10.1038/jcbfm.2011.173
38. Nadler JV, Cooper JR (1972) N-acetyl-L-aspartic acid content of human neural tumors and bovine peripheral nervous tissues. *J Neurochem* 19(2):313–319. doi:10.1111/j.1471-4159.1972.tb01341.x
39. Urenjak J, Williams SR, Gadian DG, Noble M (1992) Specific expression of N-acetylaspartate in neurons, oligodendrocyte-type-2 astrocyte progenitors, and immature oligodendrocytes in vitro. *J Neurochem* 59(1):55–61. doi:10.1111/j.1471-4159.1992.tb08875.x
40. Williams S (1999) Cerebral amino acids studied by nuclear magnetic resonance spectroscopy in vivo. *Prog Nucl Mag Res Spectrosc* 34(3–4):301–326. doi:10.1016/S0079-6565(99)00004-7
41. Narayanan S, De Stefano N, Francis GS, Arnaoutelis R, Caramanos Z, Collins DL, Pelletier D, Arnason BGW, Antel JP, Arnold DL (2001) Axonal metabolic recovery in multiple sclerosis patients treated with interferon beta-1b. *J Neurol* 248(11):979–986. doi:10.1007/s004150170052
42. Destefano N, Matthews PM, Arnold DL (1995) Reversible decreases in N-acetylaspartate after acute brain injury. *Magnet Reson Med* 34(5):721–727
43. Sonati T, Reimann RR, Falsig J, Baral PK, O'Connor T, Hornemann S, Yaganoglu S, Li B, Herrmann US, Wieland B, Swayampakula M, Rahman MH, Das D, Kav N, Riek R, Liberski PP, James MN, Aguzzi A (2013) The toxicity of anti-prion antibodies is mediated by the flexible tail of the prion protein. *Nature* 501(7465):102–106. doi:10.1038/nature12402
44. Herrmann US, Sonati T, Falsig J, Reimann RR, Dametto P, O'Connor T, Li B, Lau A, Hornemann S, Sorce S, Wagner U, Sanoudou D, Aguzzi A (2015) Prion infections and anti-PrP antibodies trigger converging neurotoxic pathways. *PLoS Pathog* 11(2):e1004662. doi:10.1371/journal.ppat.1004662